On the Validity of the Harmonic Potential Energy Surface Approximation for Nonradiative Multiphonon Charge Transitions in Oxide Defects

Y. Wimmer* W. Goes*, A.-M. El-Sayed*,†, A.L. Shluger†, and T. Grasser*
*Vienna University of Technology, †University College London, UK , Email: wimmer@iue.tuwien.ac.at

Abstract: Hole trapping in oxide defects in the gate insulator of MOSFET transistors has been linked to a wide range of phenomena like random telegraph noise, 1/f noise, bias temperature instability (BTI), stress-induced leakage current and hot carrier degradation [1–5]. Charge capture (τ_c) and emission (τ_e) times of a defect are theoretically described by nonradiative-multiphonon (NMP)-theory, where the potential energy surface (PES) along the reaction coordinate is usually approximated by a parabola [2, 6, 7]. In the classical high-temperature limit, transitions between the different charge states occur at the intersection of those parabolas, which also defines the classical reaction barrier. This harmonic approximation has been in use ever since the introduction of NMP-theory [8–10]. However,the quality of this approximation is rarely investigated [7]. In this work, we compare different approximations of the PES in order to calculate τ_c and τ_e and compare them to the results obtained by Density Functional Theory (DFT) calculations. For this we use the DFT-PES as well as two approximations of the PES of several defects to calculate τ_c and τ_e in a pMOS device. Our study covers different possible defect candidates, which have been previously identified as sources of degradation in silicon dioxide [11–13]: The oxygen vacancy (OV, see Fig. 1b) in α-quartz, the hydrogen bridge (HB, see Fig. 1c) in both α-quartz and in amorphous silicon dioxide (a-SiO_2) and the hydroxyl E' center (H-E', see Fig. 1d) in a-SiO_2. Since the amorphous structures differ from each other, also the PES varies. Therefore we have investigated 11 HB defects and 12 H-E' defects from [14] to provide statistical data. We show that the parabolic fit to the PES underestimates τ_c and τ_e by several orders of magnitude. Therefore we propose a different approximation that yields to more accurate τ_c and τ_e and captures several desired features, also in cases where the parabolic approximation fails.

Simulation Framework: For our DFT calculations we used the CP2K framework [15] with the non-local PBE0 TC LRC hybrid functional [16]. Large a-SiO_2 structures containing 243 atoms (crystalline) or 216 atoms (amorphous) were created using ReaxFF [17]. Using DFT, the defects were relaxed in their neutral and positive state. This results in slightly different atomic configurations for each charge state. The normalized reaction coordinate (NRC) is defined as the normalized atomic displacement-vector between them. For constructing the PES we used this displacement vector to interpolate configurations between the two states (range 0.0 to 1.0), or extrapolate configurations in the range -1.0 to 0.0 (or 1.0 to 2.0 respectively). The PES was then calculated by computing the energies for 30 configurations along the NRC in the range -1.0 to 2.0, and spline interpolation in between (see Fig. 2).

These PESs calculated by DFT ($\mathrm{E_{DFT}}$) were taken as a reference to evaluate the quality of possible approximations. When a gate bias is applied, the PESs shift relative to each other along the y axis, changing the reaction barrier and therebyτ_c and τ_e. In the following we will focus on these quantities, investigating whether the aforementioned approximations accurately reproduce τ_c and τ_e and their dependences. For this purpose the reaction time constants vs. gate-voltage curves (for $\mathrm{V_G} = -2.5\,\mathrm{V}$ to $2.5\,\mathrm{V}$) were calculated for each defect in a pMOS device with oxide thickness of $2.5\,\mathrm{nm}$, for different temperatures (T= 50 °C, 100 °C, 150 °C and 200 °C). For these calcualtions we use a semi-classical approach based on [9] and [18]. An example of these curves for different defects and approximations is depicted in Fig. 3.

Results and Discussion: An analytic approximation should not only be able to fit the $\tau(\mathrm{V_G})$ curves (Fig. 3 and Fig. 4) but also the dependence on the gate bias (Fig. 5) and the temperature-dependence (Fig. 6). The functions for the parabolic approximation ($\mathrm{E_{Par}}$) are usually calculated by fitting the parameter α in

$$\mathrm{E_{Par}}(q) = \alpha(q - q_0)^2 \qquad (1)$$

to two points for each parabola, with q_0 being the position of the minimum [2, 19] (see Fig. 2). However, as demonstrated in Fig. 2, $\mathrm{E_{Par}}$ tends to underestimate the crossing point. Since τ_c and τ_e are extremely sensitive to the height of this barrier [8], a good match in this region is essential for a good approximation. Very promising results were obtained using a V-approximation:

$$\mathrm{E_{Vap}}(q) = \gamma(\sqrt{1 + \beta(q - q_0)^2} - 1) \qquad (2)$$

being parabolic near the minimum at q_0 but linear for larger values of $|q - q_0|$. It should be pointed out that although we refer to this function as V-approximation this does not indicate that $\mathrm{E_{Vap}}$ has a jump discontinuity at its minimum, but rather that its shape resembles more a V than a parabola. The constant γ defines the opening angle, for simplicity reasons its value was set to 1.0 eV in this work.

Calculating τ_c and τ_e for the OV (see Fig. 3 left), $\mathrm{E_{Par}}$ actually is a very good approximation, in this case even slightly better than $\mathrm{E_{Vap}}$. However, for all the hydrogen-related defects, this is not the case and $\mathrm{E_{Par}}$ fails to reproduce the τ_c and τ_e values. Although $\mathrm{E_{Par}}$ only tends to slightly underestimate the reaction barrier (as shown in Fig. 2 left), τ_c and τ_e are lower by several orders of magnitude (Fig. 3 right). Using $\mathrm{E_{Vap}}$ the agreement improves considerably.

This observation also holds for a statistical comparison for several defects in a-SiO_2, as can be seen in Fig. 4. Correlation improves significantly when using $\mathrm{E_{Vap}}$ instead of $\mathrm{E_{Par}}$. This is valid for all five voltages presented in these plots.

The slope of the $\tau_c(\mathrm{V_G})$ curve determines the dependence of τ_c on the gate bias [2]. We determined the $\tau_c{}'(\mathrm{V_G})$ curves in the range $\mathrm{V_G} = 1.0\,\mathrm{V}$ to $2.5\,\mathrm{V}$ by a least square fit to each data set. The slope for the different approximations is again plotted in correlation-plots (Fig. 5). Like in Fig. 4 $\mathrm{E_{Par}}$ gives a poor match to the behavior calculated using $\mathrm{E_{DFT}}$, whereas $\mathrm{E_{Vap}}$ fits well. This is observed for all four temperatures investigated.

Finally, a good approximation should also be able to reproduce the temperature dependence of τ_c (the activation energy). In Fig. 6 a least square linear fit for $\tau_c(\mathrm{T})$ at $\mathrm{V_G} = 1.0\,\mathrm{V}$ is provided for the $\tau_c(\mathrm{T})$ calculated using $\mathrm{E_{DFT}}$ and both approximations discussed. Also here $\mathrm{E_{Vap}}$ reproduces the results in α-quartz and for the H-E' better than $\mathrm{E_{Par}}$. Interestingly here the fit for the HB in a-SiO_2 seams slightly worse than the parabolic approximation.

Conclusions: We have calculated τ_c and τ_e for several defects and several approximations of the PES along the reaction coordinate. By comparing them to results obtained using DFT, we show that the widely used parabolic approximation is poor for most of the investigated defects in this work, since it leads to an underestimation of τ_c and τ_e by several orders of magnitude. Furthermore it also fails to represent the slope $\tau_c{}'(\mathrm{V_G})$ or the activation energy of the DFT-results. We propose a different approximation which captures the curves in the area of interest (near the crossing point) much more accurately. This leads to a much better approximation of τ_c and τ_e and their characteristics for most of the investigated defects.

References:

[1] P. Blöchl, Phys. Rev. B **62**, 6158 (2000). **[2]** T. Grasser, Microel. Rel. **52**, 39 (2012). **[3]** T. Grasser *et al.*, (2015), (IRPS) 2015, accepted. **[4]** F. Schanovsky *et al.*, *Proc. SISPAD* (2013), pp. 1–4. **[5]** P. Lenahan *et al.*, IEEE Trans.Nucl.Sci. **48**, 2101 (2001). **[6]** A. Palma *et al.*, Phys. Rev. B **56**, 9565 (1997). **[7]** J. Ji *et al.*, *Proc. IEDM* (2014), pp. 21–4. **[8]** K. Huang *et al.*, Proc .R.Soc.A **204**, 406 (1950). **[9]** C. Henry *et al.*, Pys. Rev. B **15**, 989 (1977). **[10]** F. Schanovsky *et al.*, JCE **11**, 218 (2012). **[11]** F. Feigl *et al.*, SSC **14**, 225 (1974). **[12]** D. Griscom, Phys. Rev. B **22**, 4192 (1980). **[13]** A.-M. El-Sayed *et al.*, PRL **114**, 115503 (2015). **[14]** T. Grasser *et al.*, *Proc.(IEDM)* (2014), pp. 530–533. **[15]** B. G. Lippert *et al.*, Mol. Phys. **92**, 477 (1997). **[16]** M. Guidon *et al.*, J.Ch.Theor.Comp. **5**, 3010 (2009). **[17]** A. van Duin *et al.*, J.Ph.Chem.A **105**, 9396 (2001). **[18]** F. Schanovsky, Ph.D. thesis, 2013. **[19]** W. Gös *et al.*, *Bias Temp. Inst. for Dev. and Circ.*, edited by T. Grasser (Springer, 2013), pp. 409–446.

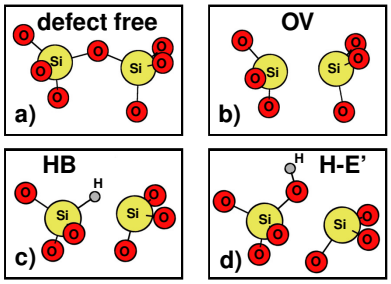

Fig. 1: Schematics of the different defects (b,c,d) used for the calculations compared to the defect-free structure (a). In the oxygen vacancy (b) an O-atom is missing, while for the hydrogen bridge (c) it is replaced by a H-atom. In the case of the hydroxyl E' center (d) a H-atom is bound to the O-atom having broken up one of the Si-O bonds. The latter defect needs bond distances larger than 1.65A [14] which are not present in α-quartz and therefore does only exist in amorphous structures.

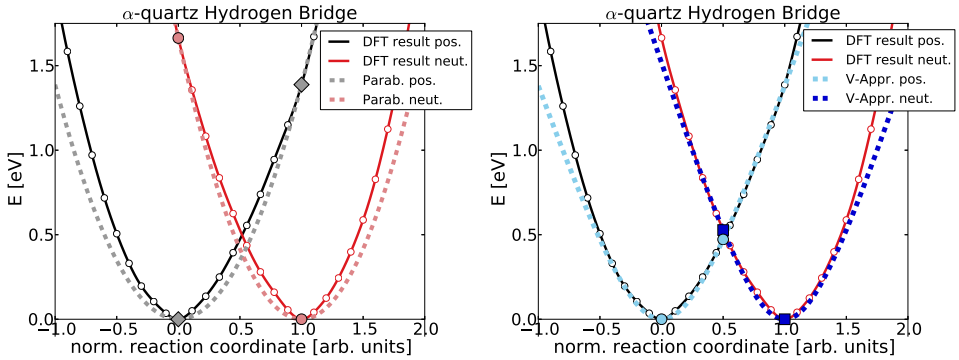

Fig. 2: Cut through the potential energy surface along the norm. reaction coordinate for the neutral to the positive state of the hydrogen bridge (see Fig. 1 c) in α-quartz and the two different approximation variants discussed in this paper. In the parabolic approximation (left), the neutral PES (grey) is constructed using (1) fitted to the two grey points. These points are the value of the neutral PES at the neutral configuration and at the positive configuration when charged neutrally. The positive PES is constructed in a similar way.
The V-approximation (2)(right) represents the E_{DFT} near the intersection point much better. Taking the neutral PES (light blue) as an example, one can see that here the points at 0.0 and 0.5 on the norm. reaction coordinate are used for the approximation. When a voltage is applied, the PESs shift relative to each other along the y axis, changing the intersection point which defines the reaction barrier in the classical high-temperature limit.

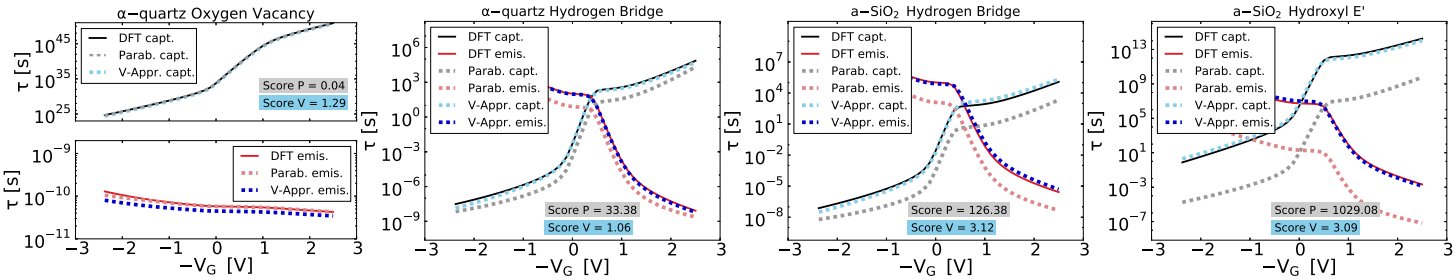

Fig. 3: Depending on the applied bias conditions, the PESs in Fig. 2 move up or down changing the energy-barrier that has to be overcome for charge-capture or emission. The above plots show the reaction time-constants τ_c and τ_e at T=100°C. It can be seen that they are very sensitive to a change of the barrier height. Although the parabolic approximation is good for the oxygen vacancy (left) (even slightly better than the V-approximation), it fails by several orders of magnitude for all the hydrogen-related defects (right). For the defects in a-SiO_2, the behavior of $\tau_c(V_G)$ ($\tau_e(V_G)$) is of course slightly different for each investigated structure. The two respective graphs are examplary for one of the investigated structures. One can see a considerable improvement when the V-approximation (2) is used. To quantify the improvement, a l^2 norm for $\log(\tau_c(\mathrm{DFT}))$-$\log(\tau_c(\mathrm{appr.}))$ (similar for τ_e) is shown as score function.

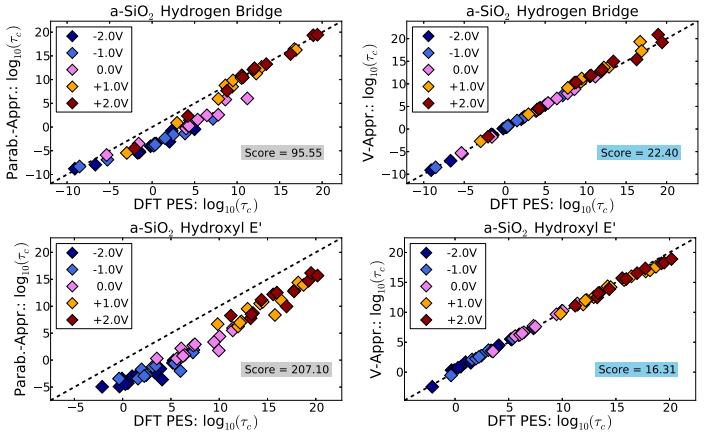

Fig. 4: Double logarithmic correlation-plots for the absolute values of τ_c at T=100°C for the hydrogen bridge in a-SiO_2 (top) and hydroxyl E' center (bottom). Correlation of τ_c calculated using E_{DFT} and τ_c calculated using E_{Par} (left) or E_{Vap} (right) are shown. When τ_c for both approximations is the same, the respective point would lie along the diagonal, therefore the off-diagonality can be used as a criterion determining the quality of the fit. It is clearly visible that τ_c tends to be underestimated in the parabolic approximation. To quantify the improvement a l^2 norm for the distance to the diagonal is shown as a score function.

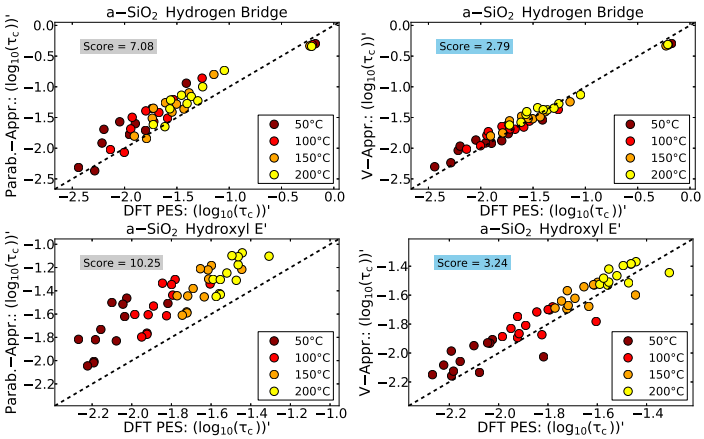

Fig. 5: Correlation-plots for the slope of $\log_{10}(\tau_c(V_G))$. Like in Fig. 4, the hydrogen bridge in a-SiO_2 is depicted on top and the hydroxyl E' center at the bottom. Correlation of τ_c' calculated using E_{DFT} and τ_c' calculated using E_{Par} (left) or E_{Vap} (right) are shown. It is clearly visible that $\tau_c'(V_G)$ is overestimated in the parabolic approximation. Also, to quantify the improvement, a l^2 norm for the distance to the diagonal is shown as a score function.

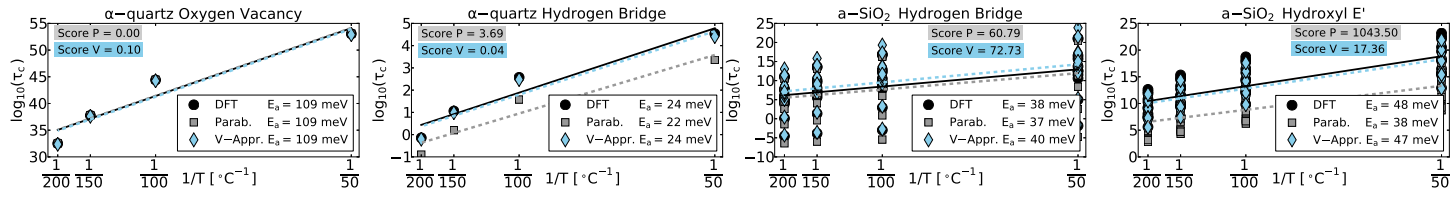

Fig. 6: Arrhenius plots showing the temperature dependence of $\tau_c(T)$ at V_G = 1.0 V in the four investigated defects. In the amorphous structures, the values are distributed over a wide range. The lines are a least square fit to the data points, also providing the slope to calculate the activation energy E_a. To quantify the improvement, a l^2 norm for the differences to the results using E_{DFT} (black) is depicted as score function. For the case of the HB in α-quartz and for the H-E', E_{Vap} (light blue) is a better approximation than E_{Par} (grey). Interestingly, for the HB in a-SiO_2 the score for E_{Vap} is slightly worse.